



**AUSTRALIAN ATOMIC ENERGY COMMISSION
RESEARCH ESTABLISHMENT
LUCAS HEIGHTS**

**EXPOSURE CALIBRATION OF A THIMBLE CHAMBER BY
CALORIMETRIC AND IONIMETRIC METHODS**

by

**D.F. URQUHART
E.P. JOHNSON
W.S. BADGER**

August 1973

ISBN 0 642 99597 4

AUSTRALIAN ATOMIC ENERGY COMMISSION
RESEARCH ESTABLISHMENT
LUCAS HEIGHTS

EXPOSURE CALIBRATION OF A THIMBLE
CHAMBER BY CALORIMETRIC AND
IONIMETRIC METHODS

by

D.F. Urquhart

E.P. Johnson

W.S. Badger

ABSTRACT

A Baldwin-Farmer thimble chamber, fitted with a perspex build-up cap was calibrated against an absolute graphite cavity chamber to provide an interim working standard of exposure for ^{137}Cs and ^{60}Co photons. The calibration factor (roentgens per coulomb) at ^{60}Co energy was 2% higher than an NPL, 2MV calibration for this chamber, carried out in the UK by the National Physical Laboratory.

The thimble chamber, fitted with an aluminium build-up cap, was also used to make a comparison between the graphite cavity chamber and an aluminium micro-calorimeter which is to be used as an interim absorbed dose standard. Exposure calibration factors for the thimble chamber derived from calorimeter measurements were in good agreement with calibration factors derived from cavity chamber measurements, at both ^{137}Cs and ^{60}Co energies.

National Library of Australia card number and ISBN 0 642 99597 4

The following descriptors have been selected from the INIS Thesaurus to describe the subject content of this report for information retrieval purposes. For further details please refer to IAEA-INIS-12 (INIS: Manual for Indexing) and IAEA-INIS-13 (INIS: Thesaurus) published in Vienna by the International Atomic Energy Agency.

ACCURACY; ALUMINIUM; ATTENUATION; CALIBRATION; CALORIMETERS;
CESIUM 137; COBALT 60; COMPARATIVE EVALUATIONS; CORRECTIONS;
DATA; ELECTRIC CURRENTS; GAMMA RADIATION; GRAPHITE; IONIZATION
CHAMBERS; RADIATION DOSES; RADIATION QUALITY

CONTENTS

	Page
1. INTRODUCTION	1
2. THE IRRADIATION CELL	2
3. THE GRAPHITE CAVITY CHAMBER	2
4. THE BALDWIN-FARMER CHAMBER	2
5. MEASUREMENT OF IONISATION CURRENT	3
6. THE ALUMINIUM CALORIMETER	3
7. IONIMETRIC EXPOSURE CALIBRATION OF THIMBLE CHAMBER	5
8. CALORIMETRIC CALIBRATION OF THE THIMBLE CHAMBER	6
9. RADIATION QUALITY AND THE ENERGY RESPONSE OF THE THIMBLE CHAMBER	8
9.1 The Spectra of Scattered Radiation from the Teletherapy Unit	8
9.2 Photon Scattering in the Front Wall of the Calorimeter	9
9.3 Energy Response of the Thimble Chamber	9
10. ACCURACY OF MEASUREMENTS AND CONCLUSIONS	10
11. ACKNOWLEDGEMENTS	11
12. REFERENCES	11
Table 1	Comparison of the Aluminium and Graphite Calorimeters
Table 2	The Irradiation Cell - Useful Range of Irradiation Conditions
Table 3	The Aluminium Calorimeter - Characteristics
Table 4	¹³⁷ Cs Source. Measured Values of Current, $I(x)$, and Exposure, $X(x)$, Using the Graphite Cavity Chamber
Table 5	⁶⁰ Co Source. Measured Values of Current, $I(x)$ and Exposure, $X(x)$, Using the Graphite Cavity Chamber
Table 6	Measured Current, $I_t(x)$ for Baldwin-Farmer Chamber (No. 617030)
Table 7	Exposure Calibration Factor, N , for Baldwin-Farmer Chamber (No. 617030)
Table 8	¹³⁷ Cs Source, Measured Values of Dose, $D(x,d)$ and Thimble Chamber Current, $I_t(x,d)$, in Aluminium
Table 9	⁶⁰ Co Source. Measured Values of Dose, $D(x,d)$, and Thimble Chamber Current, $I_t(x,d)$, in Aluminium
Table 10	Accuracy of Ionimetric Calibration of the Thimble Chamber
Table 11	Accuracy of Calorimetric Calibration of the Thimble Chamber

CONTENTS (Cont'd.)

- Figure 1 Plan of irradiation cell.
- Figure 2 Radiograph of aluminium calorimeter
- Figure 3 Block diagram of calorimeter temperature measurement and control system.
- Figure 4 Graphite cavity chamber.
- Figure 5 Block diagram of Townsend balance.
- Figure 6 Energy response of the Baldwin-Farmer Chamber with the perspex cap.
- Figure 7 Energy response of the Baldwin-Farmer Chamber with the aluminium cap.
- Appendix A - Definitions of Symbols and Terms
- Appendix B - Evaluation of the Correction Factors, Coefficients and Constants
- Appendix C - The Mean Energy of the Photon Spectrum at the Calorimeter Absorber

1. INTRODUCTION

Part of the Australian Atomic Energy Commission's radiation standards programme is the development of exposure and absorbed dose standards for photons above 300 keV energy. The primary standard instruments proposed for this are a graphite calorimeter for absorbed dose and an absolute graphite cavity chamber for exposure. The graphite calorimeter has been designed and the parts are being manufactured; the graphite cavity chamber has yet to be designed.

While these two instruments are being made, it is proposed to set up interim working standards for absorbed dose and exposure using two existing absolute instruments for primary standards, and a Baldwin-Farmer thimble chamber as a practical (calibrated) working standard. One of the absolute instruments is an aluminium calorimeter, made primarily to test temperature measurement and control systems, and construction methods to be used for the graphite calorimeter. Although this is a cruder instrument it can provide absorbed dose standards at dose rates above 10 rad min^{-1} to an absolute accuracy of better than 2%. The main features of the two calorimeters are compared in Table 1. The second absolute instrument is a parallel plate graphite ionisation chamber in which the collecting volume can be determined from direct measurements of the electrode spacing and the diameter of the collector.

The objectives of this work were threefold:

- (1) To make an 'exposure in air' calibration of a Baldwin-Farmer Thimble Chamber (No.617030), fitted with a perspex build-up cap, at ^{137}Cs and ^{60}Co energies. This was done using the graphite cavity chamber as the primary standard.
- (2) To measure the 'agreement' between the calorimeter and the cavity chamber. This was done by comparing two exposure calibrations of the Baldwin-Farmer chamber, fitted with an aluminium build-up cap, at ^{137}Cs and ^{60}Co energies. In one calibration the calorimeter was used as the primary standard and in the other the cavity chamber was used as the primary standard.
- (3) To compare these calibration measurements with the only external standard at present available. This is a 2 MV exposure calibration of the Baldwin-Farmer Chamber (No.617030) which was made in the UK by the National Physical Laboratory (NPL).

Definitions of the symbols and terms used in this report are given in Appendix A.

The calibration of the Baldwin-Farmer chamber for absorbed dose in water, using the aluminium calorimeter as the primary standard, will be reported elsewhere.

2. THE IRRADIATION CELL

The ^{137}Cs and ^{60}Co measurements were made in the irradiation cell shown in Figure 1. An Eldorado 6 teletherapy unit made by Atomic Energy of Canada Ltd., is used to provide a well collimated beam with easily adjustable field size. The two sources at present available for use in this machine are a 1.4 kCi ^{137}Cs source (with low ^{134}Cs content) and a 3.4 kCi ^{60}Co source. The caesium source was also obtained from Atomic Energy of Canada Ltd; the dimensions of the active source material are 25.0 mm dia. x 38.2 mm. The cobalt source was supplied by the Isotope Division of the AAEC and has active source dimensions of 17 mm dia. x 16 mm. Each source is contained in a stainless steel capsule with wall thickness of approximately 1 mm. Beam traps in the cell wall and floor enable the use of horizontal or vertical beams. The approximate ranges of exposures and irradiation geometries available with this facility are shown in Table 2.

3. THE GRAPHITE CAVITY CHAMBER

This chamber (Figure 4) is made of AG type graphite with a density of $1.375 \pm 0.003 \text{ g cm}^{-3}$. The thickness of the front wall of the chamber can be varied to determine corrections for lack of electronic equilibrium and photon attenuation. The collecting volume is $910.1 \pm 2.0 \text{ mm}^3$ and the effective collecting volume is $910.1 \pm 4.0 \text{ mm}^3$, including a possible error due to field nonuniformity, calculated by the method of Barber (1961) to be not greater than 0.2%.

This chamber (R.M. Fry, AAEC unpublished report) was designed for a different purpose and later was modified (D.R. Davy and J.W. Griffiths, AAEC unpublished report) for use as an exposure standard. Further modifications have been made by the authors of this report.

4. THE BALDWIN-FARMER CHAMBER

The Baldwin-Farmer chamber was purchased from Isotopes Development Ltd., UK with a removable perspex build-up cap (4.5 mm wall thickness); also supplied was an NPL report on the calibration of the chamber (with the build-up cap). The reported calibration factor (dated 3.5.68) was $5.46 \times 10^9 \text{ R C}^{-1}$ for dry air at 22°C and 760 mm Hg. The calibration was done using 2 MV X-rays (HVL: 12 mm Cu) at an exposure rate of 12 R min^{-1} , a 5 cm dia. field size, and a chamber polarising potential of -180 volt. In accordance with the prevailing NPL policy no statement of accuracy was given in the calibration report.

A second build-up cap was made for this chamber using the same type of aluminium alloy as the calorimeter; this cap has a wall thickness of approximately 1.90 mm or 0.55 g cm^{-2} .

5. MEASUREMENT OF IONISATION CURRENT

Ionisation currents in both chambers were measured on a Townsend balance system developed at the AAEC Research Establishment (D.R. Davy, R.M. Fry and J.W. Griffiths, AAEC unpublished report). In this system (Figure 5), the current to be measured charges a known capacitor, C, and the developed voltage is balanced by a voltage ramp whose slope is adjusted manually to match the charge rate of the capacitor. Lack of balance is detected by an EIL model 33c Vibron Electrometer. At the end of a timed charging period (Δt) the ramp voltage (V) is measured by a 6-digit Solartron LM 1867C digital voltmeter (input resistance greater than $10^{10} \Omega$). The ionisation current (I) is then calculated using the equation

$$I = \frac{CV}{\Delta t} .$$

The calibration of the digital voltmeter is checked daily against an internal unsaturated Weston reference cell. The internal calibration voltage is checked monthly against an external, temperature controlled, saturated standard cell (Muirhead type K-231 - A) with a certified e.m.f. traceable to the National Physical Laboratory Volt of Great Britain.

The value and temperature coefficient of the capacitor were measured using a General Radio Company a.c. bridge, type 1615-A and reference Standard Capacitor, type 1404, traceable to the US National Bureau of Standards Standard Farad.

6. THE ALUMINIUM CALORIMETER

The calorimeter is a quasi-adiabatic type similar in principle to those described by Milvy et al. (1958), Genna et al. (1963) and Engelke and Hohlfield (1971). Some of the advantages of this type of calorimeter have been discussed elsewhere (Urquhart 1971). A radiograph of the calorimeter in plan is shown in Figure 2. Figure 3 contains a block diagram of the complete instrument.

The aluminium absorber has a total mass of $13.546 \pm 0.04 \text{ g}$, including 0.152 g of epoxy cement and 0.018 g of other foreign material, nichrome wire, copper wire, and two miniature bead thermistors.

The jacket surrounding the absorber is free to rise in temperature during an irradiation, and can be heated electrically at the same rate as the absorber during a calibration. The temperature of the mantle surrounding the

jacket is controlled to about 26°C and is constant to within $\pm 2 \times 10^{-5} \text{ }^{\circ}\text{C}$. During irradiation or calibration the mantle temperature may be increased by manual adjustment of the temperature control bridge to match the rise in the jacket and absorber. This rise is generally between 10^{-3} and $10^{-2} \text{ }^{\circ}\text{C}$. The temperature of the aluminium vacuum chamber housing the calorimeter is maintained at about 25°C and is constant to within $\pm 2 \times 10^{-2} \text{ }^{\circ}\text{C}$. The room temperature is kept within the range 21 to 24°C .

Changes in the absorber temperature are registered on a 100 mV potentiometric strip chart recorder (chart width 280 mm). The out-of-balance voltage on the temperature sensing d.c. bridge, required to produce a full scale deflection on the recorder, can be varied by the range switch on the Keithley 147 nanovolt null detector used to drive the recorder. Performance figures for the $1 \mu\text{V}$ range and a bridge voltage of 18 volts are shown in Table 3. The 'bridge only' values in Table 3 were obtained by replacing the temperature sensing thermistor with a manganin wire-wound resistor of equal value. Errors due to heating of the thermistor by the bridge supply voltage (18 volts) were calculated by the method of Laughlin and Genna (1956) to be less than 0.01%. The power delivered to the absorber during calibration was determined by making two voltage measurements, using the digital voltmeter cited in Section 5. One measurement, V_a (mV), was made across the heater resistance (approximately 770Ω) and the other, V_s (mV), across a precision, manganin wire-wound resistor connected in series with the heater. This resistor is a Leeds and Northrup SR type with a value of $770.0 \pm 0.4 \Omega$. The power P_a delivered to the absorber was then given by

$$P_a = V_a \cdot V_s / 770.0 \text{ (}\mu\text{W)} .$$

Minor corrections to this equation are discussed in Appendix B Section B2.

Each absorbed dose measurement is essentially a comparison of the heating rate produced by the radiation in a known mass of aluminium (e.g. the absorber) with the heating rate produced by a measured amount of electrical power in the same mass. The 'comparator' system consists of four components - thermistor, bridge, null detector and recorder. If it is assumed that all the energy absorbed from the radiation beam by the absorber is converted to thermal energy, the absolute accuracy of the calorimeter depends, in principle, on three factors:

- (i) the measurement of the mass of the absorber,
- (ii) the measurement of electrical power delivered to the absorber during calibration, and
- (iii) the stability of the comparator over the time interval between

radiation heating and electrical calibration.

The absorber mass was measured on a Mettler B6 balance whose calibration is traceable ultimately to a national standard kilogram.

The calibration power is measured in terms of a precision resistor (traceable to a national standard ohm) and a standard cell (traceable to a national standard volt).

The stability of the comparator depends essentially on the stability of the recorder sensitivity, the gain stability of the null detector and the stability of the temperature coefficient of the thermistor. The longest interval between the start of an irradiation and the start of the associated electrical calibration is about 60 minutes, but generally the interval is less than 30 minutes.

Drift in sensitivity of the bridge - null detector - recorder sections of the system can be measured separately by replacing the thermistor arm of the bridge with a fixed resistance and observing the recorder chart deflection when a fixed step change is made in one arm of the bridge by means of a decade resistance box. Changes in sensitivity were barely detectable over periods of several hours and amounted to less than 1% of full scale chart deflection over 3 to 4 weeks, with 18 volts on the bridge and using the 1 μ V range on the null detector.

It is difficult to measure separately the instability of the thermistor, but there is no evidence of any significant changes with time. The measured change in the resistance of the thermistor arm of the bridge per unit of electrical energy input to the absorber has changed by less than 2% over a period of more than 8 months. The overall stability of the comparator is also reflected in the standard deviations for measurements of chart deflection per joule of electrical heat input (Tables 8 and 9, column 4) repeated over periods of three or four days.

7. IONIMETRIC EXPOSURE CALIBRATION OF THE THIMBLE CHAMBER

The Baldwin-Farmer chamber, fitted with its perspex cap, was calibrated by placing it centrally in the beam at a distance, x , from the source. The saturated chamber current, $I_t(x)$ (ampere), was measured at time t_0 and corrected to 22°C and 760 mm Hg. If the exposure rate in air at t_0 is $\Delta X(x)/\Delta t$ ($C\ kg^{-1}s^{-1}$) at this point, then the calibration factor N for the chamber is given by:

$$N = \frac{\Delta X(x)}{\Delta t} / (2.58 \times 10^{-4} \cdot I_t(x) \cdot k_1 \cdot k_2 \cdot k_{32}) \cdot R\ C^{-1} \quad \dots(1)$$

where k_1 , k_2 , k_{32} are small corrections described in Appendix B.

The exposure rate $\Delta X(x)/\Delta t$ was measured by placing the graphite cavity chamber at the same point and measuring the saturated chamber current, $I(x,d)$ (ampere), at t_0 (at 0°C and 760 mm Hg), and the front wall thickness d_w .

The exposure rate is then given by:

$$\frac{\Delta X(x)}{\Delta t} = \frac{I(x) \cdot \bar{S}_m \cdot k_1 \cdot k_2}{v \cdot \rho_0} = \frac{I(x,d) \cdot k_w \cdot \bar{S}_m \cdot k_1 \cdot k_2}{v \cdot \rho_0} \cdot C \text{ kg}^{-1} \text{ s}^{-1} \quad \dots (2)$$

where

- $I(x)$ = the current in an ideal cavity chamber with full electronic equilibrium and zero front wall attenuation (at 0°C and 760 mm Hg);
- \bar{S}_m = the mean mass stopping power ratio (relative to air) for the medium;
- v = the effective collecting volume of the chamber;
- ρ_0 = the density of dry air at 0°C and 760 mm Hg;
- k_w = $[\exp(-\mu d_w) (1 + \sin a \cdot d_w) - \exp(-\beta \cdot d_w)]^{-1}$
- = the correction for lack of electronic equilibrium and attenuation in the front wall (Barnard et al. 1959, 1962, 1964),
- where

- μ = the linear attenuation coefficient for photons in the medium,
- a = a linear photon scatter coefficient, and
- β = a linear attenuation coefficient for secondary electrons.

In practice $I(x,d)$ is measured for several front wall thicknesses and a mean value $\bar{I}(x)$ used to calculate $\Delta X(x)/\Delta t$.

Details of measurements of $I(x,d)$, $I_t(x)$ and calculated values of k_w , $I(x)$ and N are given in Tables 4 to 7 for ^{137}Cs and ^{60}Co .

Values of all minor correction factors, k_0 , k_1 , k_2 , k_{20} , k_{21} , k_{30} , k_{31} , k_{32} and values of coefficients and constants in Equation (2) are shown in Appendix B.

The Baldwin-Farmer chamber fitted with the aluminium cap was calibrated in the same way.

8. CALORIMETRIC CALIBRATION OF THE THIMBLE CHAMBER

The Baldwin-Farmer thimble chamber, fitted with the aluminium build-up cap was, calibrated by inserting it into a cavity in a dummy of the aluminium calorimeter with its centre at a distance, x from the source and at depth, d , in aluminium. The saturated ionisation current, $I_t(x,d)$ (ampere), at time t_0 and at 22°C and 760 mm Hg, was measured in this position. If the exposure rate

was $\Delta X(x,d,r)/\Delta t$ ($C \text{ kg}^{-1} \text{ s}^{-1}$) at the centre of the air filled cavity, radius r , made to accommodate the chamber, then the calibration factor, N is given by:

$$N = \frac{\Delta X(x,d,r)}{\Delta t} / (2.58 \times 10^{-4} I_t(x,d) \cdot k_1 \cdot k_2 \cdot k_{33} \cdot k_{34}) \cdot R C^{-1} \quad \dots (3)$$

where k_{33} , k_{34} are minor corrections described in Appendix B.

The exposure $X(x,d,r)$ was derived from a measurement of the absorbed dose $D(x,d)$ in aluminium, at distance x and depth d , by the calorimeter.

First the exposure in a small cavity at depth d , $X(x,d)$, was found using the following relationship, (ICRU 1962):

$$\frac{\Delta X(x,d)}{\Delta t} = \frac{\Delta D(x,d)}{\Delta t} \cdot \frac{1}{\bar{W}} \cdot \frac{(\mu_{en}/\rho)_{\text{air}}}{(\mu_{en}/\rho)_{\text{Al}}} \cdot k_1 \cdot k_2 \cdot k_{10} \cdot k_{11} \cdot k_{12}, \quad \dots (4)$$

where k_{10} , k_{11} , k_{12} are small corrections described in Appendix B, and where

\bar{W} = the average energy required to produce an ion pair in air,

$(\mu_{en}/\rho)_{\text{air}}$ = the mass energy absorption coefficient for air,

$(\mu_{en}/\rho)_{\text{Al}}$ = the mass energy absorption coefficient for aluminium.

If the size of the air cavity is increased to a finite radius r , which is just large enough to accommodate the thimble chamber and cap (keeping $(d-r)$ large enough to maintain electronic equilibrium), then the exposure is increased by a displacement factor k_d , due to the reduced attenuation; thus

$$\frac{\Delta X(x,d,r)}{\Delta t} = k_d \cdot \frac{\Delta X(x,d)}{\Delta t}, \quad \dots (5)$$

The evaluation of the displacement factor and other constants and coefficients used in Equations (4) and (5) is given in Appendix B.

The observed absorbed dose rate $\Delta D(x,d)/\Delta t$ was found from the basic calorimeter equation:

$$\frac{\Delta D(x,d)}{\Delta t} = \frac{\Delta T(x,d)}{\Delta t} \cdot \frac{1}{m} \cdot \frac{\Delta E}{\Delta T}, \quad \dots (6)$$

where

$\frac{\Delta T(x,d)}{\Delta t}$ = the observed value of the calorimeter radiation heating rate, shown in Tables 8 and 9 in units of millimetres of recorder chart deflection per second,

$\frac{\Delta E}{\Delta T}$ = the response to electric calibration as shown in Tables 8 and 9 in units of joule per metre of recorder chart deflection, and

m = the mass of calorimeter absorber.

Values of the calibration factor N , for the ^{137}Cs and ^{60}Co sources, obtained by using Equations (3) to (6), are shown in Table 7, column 6.

9. RADIATION QUALITY AND THE ENERGY RESPONSE OF THE THIMBLE CHAMBER

In determining the absorption, attenuation and scatter coefficients, the radiation emitted by the teletherapy unit was assumed to be monoenergetic - 1.25 MeV for ^{60}Co and 0.66 MeV for ^{137}Cs . In fact, the radiation from both sources must contain a low energy component due to backscatter from the source housing, forward scatter in the source and collimator, and possibly Bremsstrahlung radiation produced by the slowing down of beta particles in the source. Further degradation of the radiation reaching the calorimeter absorber is caused by scattering in the thick front wall of the calorimeter.

No measurements of radiation quality have yet been made for these sources. Since a good knowledge of the radiation spectra is required to make accurate corrections for such measurements, it was decided to determine the coefficients referred to above on the basis of monoenergetic radiation, but to make the accuracy limits wide enough to allow for the maximum errors which could reasonably be incurred in this way. Rough estimates of effective photon energies are good enough for this.

Estimates of effective photon energies are also required to allow for the energy dependence of the thimble chamber when comparing exposure calibrations made at different radiation qualities.

9.1 The Spectra of Scattered Radiation from the Teletherapy Unit

Qualitatively, the most significant contribution to the scattered spectrum must be from photons backscattered from material in the source housing immediately behind the source. From the Compton energy-angle relationship the energy of photons scattered through 180° is about 210 keV for ^{60}Co and 185 keV for ^{137}Cs . Multiple scattering will give rise to a continuum between the backscatter energy and the primary energy, and scattering from the collimator will be mainly small angle scattering producing only small reductions in photon energy resulting in a 'tail' on the primary photon peak.

These features can be seen in experimental results obtained by Scrimger and Cormack (1963) and Aitken and Henry (1964), in the theoretical studies by Cormack and Johns (1958), and in the unpublished work of M.J. Berger, each of which has been summarised in ICRU (1970). The Monte Carlo calculations of Berger show that in thick caesium sources the backscatter peak is flattened because of internal self-absorption. The result is a scatter spectrum which is essentially flat from the primary energy down to the backscatter energy where it drops off rapidly.

Using the Monte Carlo calculations of Berger it was estimated that scattered radiation with a mean energy of about 0.3 MeV contributed about 10%

of the output of our ^{60}Co source. On this basis the mean source energy is 1.16 MeV with an estimated uncertainty of ± 0.04 MeV. Jones (1961) has made HVL measurements for a ^{60}Co therapy source which indicate an effective energy of 1.12 to 1.15 MeV.

Using Berger's calculations, radiation from our caesium source was estimated to contain about 15% scattered radiation with a mean energy of about 0.4 MeV, giving a mean source energy of 0.62 ± 0.04 MeV.

9.2 Photon Scattering in the Front Wall of the Calorimeter

The calculations given in Appendix C, indicate that the mean energy of the primary component of the beam is reduced by about 6.5% (for both ^{60}Co and ^{137}Cs) in traversing the front wall of the calorimeter. If the mean energy of the scattered component of the beam is reduced by the same amount, the mean energy of photons reaching the calorimeter absorber is about 1.08 MeV for ^{60}Co and about 0.58 MeV for ^{137}Cs . These figures are likely to be too high because the scatter coefficients used in the calculations of Appendix C are probably too low (see Appendix B, Section B5). The accuracy limits placed on these estimates of mean energy are $+ 0.04$, $- 0.07$ MeV.

9.3 Energy Response of the Thimble Chamber

To compare calibrations of the thimble chamber made by the graphite cavity chamber, the calorimeter and by NPL, the energy response of the thimble chamber should be considered.

The thimble chamber was therefore calibrated against the graphite cavity chamber at two additional points with effective energies of 128 keV and 1.08 MeV. The lower energy was obtained using a 250 kV X-ray machine with a hard filter, which produced a half-value layer of 2.58 mm Cu. The field size and source to detector distance used for the X-ray measurements were approximately the same as those for the ^{137}Cs , ^{60}Co calibrations. The 1.08 MeV point was obtained by using the ^{60}Co source and interposing a 27.6 mm thick aluminium plate between the source and the chamber, close to the chamber. This degrades the ^{60}Co spectrum in the same way as the thick front wall of the calorimeter and produces an effective energy of about 1.08 MeV (see Section 9.2).

Although there are not enough calibration points available to determine precisely the thimble chamber energy response, the general trend is indicated by the smooth curves drawn through the four calibrations made against the graphite cavity chamber in Figure 6 (with perspex cap) and Figure 7 (with aluminium cap).

The vertical error bars in these figures are total absolute errors containing a large systematic component common to all calibrations made with

the cavity chamber. The horizontal error bars indicate the estimated degree of uncertainty in the effective energies at which the calibrations were made.

The calibration factors obtained in these additional measurements were as follows:

Source	Effective Energy (MeV)	Calibration Factor, N	
		Perspex Cap (GR C ⁻¹)	Aluminium Cap (GR C ⁻¹)
250 kV X-rays	0.128	6.55	6.59
	±0.03	±0.38	±0.38
Degraded	1.08	5.51	5.34
⁶⁰ Co	+0.04	±0.25	±0.25
	-0.07		

10. ACCURACY OF MEASUREMENTS AND CONCLUSIONS

The overall accuracies of the ionimetric and calorimetric calibrations of the Baldwin-Farmer chamber are shown in Table 7 and the contributions to these errors from various sources are listed in Tables 10 and 11. In assessing total errors, random errors were summed by taking the square root of the sum of the squares of the individual errors and adding to it the algebraic sum of the systematic errors.

From the results shown in Table 7 it can be seen that 2 MV calibration carried out by NPL is about 2% below the graphite cavity chamber calibration at ⁶⁰Co energy. This error may be due partly to the differences in radiation quality indicated by the tentative energy response curve for the thimble chamber in Figure 6.

This result is well within our own limits of accuracy; the accuracy of the NPL value is not stated.

From the figures shown in Table 7, the calorimeter calibration appears to differ from the cavity chamber calibration by about 1% for the ⁶⁰Co source and 2% for the ¹³⁷Cs source. The agreement is nearer to 0.5% for both ¹³⁷Cs and ⁶⁰Co if the curve of Figure 7 is a true indication of the energy response of the thimble chamber. In any case the agreement is well within our limits of absolute accuracy.

It is proposed that the Baldwin-Farmer Thimble Chamber (No.617030) with perspex cap be used as an interim AAEC working standard for exposure to ⁶⁰Co and ¹³⁷Cs radiation and that the values for these energies be taken as the

current values for the calibration factors (see Table 7, column 3). These values can be checked from time to time against the cavity chamber.

It is also proposed that the Baldwin-Farmer Thimble Chamber be established as an interim AAEC working standard for absorbed dose in water by calibrating it against the aluminium calorimeter. This proposition will be the subject of a later report.

11. ACKNOWLEDGEMENTS

The assistance given by several individuals and groups has been greatly appreciated. Thanks are therefore extended to the AAEC workshops for construction of the parts for the calorimeter; the AAEC Instrumentation and Control Division for the design and construction of d.c. amplifiers for temperature control; the AAEC Chemical Technology Division for analysis of materials used for the calorimeter and cavity chamber and the AAEC Isotope Division for supplying and installing the ^{60}Co source. Mr. D. Davy was available for helpful discussions and Mr. J.W. Griffiths gave valuable work in the assembly of the calorimeter.

12. REFERENCES

- Aitken, J.H., Henry, W.H. (1964) - Spectra of the internally scattered radiation from large ^{60}Co sources used in teletherapy. *Int. J. Appl. Radiat. Isotop.* 15, 713.
- Barber, B. (1961) - The basic design data of a guarded-field thimble ionisation chamber - further analytical investigations. *Phys. Med. Biol.* 6, 389.
- Barnard, G.P., Axton, E.J., Marsh, A.R.S. (1959) - A study of cavity ion chambers for use with 2 MV X-rays: equilibrium wall thickness: wall-absorption correction. *Phys. Med. Biol.* 3, 366.
- Barnard, G.P., Axton, E.J., Marsh, A.R.S. (1962) - On the use of roentgen-calibrated, cavity-ionisation chambers in tissue-like phantoms to determine absorbed dose. *Phys. Med. Biol.* 7, 229.
- Barnard, G.P., Marsh, A.R.S., Hitchman, D.G.I. (1964) - Studies of cavity ionisation chambers with mega voltage X-rays. *Phys. Med. Biol.* 9, 295.
- Cormack, D.V., Johns, H.E. (1958) - Spectral distribution of scattered radiation from a kilocurie cobalt-60 unit. *Brit. J. Radiol.* 31, 497.
- Evans, R.D. (1968) - X-ray and γ -ray interactions. *Radiation Dosimetry vol. I*, 2nd ed. p.93. Edited by F.H. Attix and W.C. Roesch. Academic Press.
- Engelke, B.A., Hohlfield, K. (1971) - A calorimeter designed for standard measurements of absorbed dose and the determination of average

- energy expended in air to produce one ion pair. PTB - Mitteilungen 5/71, p.336. AAEC-LIB/Trans. 425 (tr. P.J.F. Newton).
- Genna, S., Jaeger, R.G., Nagl, J., Sanielevici, A. (1963) - Quasi-adiabatic calorimeter for the direct determination of radiation dose in rad. At. Energy. Rev. 1, 239.
- Greening, J.R. (1964) - Saturation characteristics of parallel-plate ionisation chambers. Phys. Med. Biol. 9, 143.
- ICRU (1962) - Physical aspects of irradiation. Report 10b.
- ICRU (1968) - Radiation quantities and units. Report 11.
- ICRU (1970) - Specification of high activity gamma-ray sources. Report 18.
- Jones, D.E.A. (1961) - The suitability of materials used for the measurement of the half-value thickness of X-ray beams. Brit. J. Radiol. 34, 801.
- Lauchlin, J.S., Genna, S. (1956) - Calorimetric Methods. Radiation Dosimetry, Edited by G.J. Hine and G.L. Brownell, p.431. Academic Press N.Y.
- Loftus, T.P., Petree, B., Weaver, J.T. (1966) - The effect of humidity on ionisation measurements with cavity and free air chambers. Radiology 86, 149.
- Milvy, P., Genna, S., Barr, N., Laughlin, N.S. (1958) - Calorimetric determination of local absorbed dose. Proc. 2nd U.N. Conf. on the Peaceful Uses of Atomic Energy. Pt. 21, p.142.
- Nelms, A.T. (1953) - Graphs of the Compton energy-angle relationship and the Klein-Nishina formula from 10 keV to 500 MeV. NBS circular No.542.
- Scrimger, J.W., Cormack, D.V. (1963) - Spectrum of the radiation from a cobalt-60 teletherapy unit. Brit. J. Radiol. 36, 514.
- Urquhart, D.F. (1971) - Calorimetry - the AAEC programme. Australas.Bull. Med. Phys. Biophys. No.49, p.3.

TABLE 1
COMPARISON OF THE ALUMINIUM AND GRAPHITE CALORIMETERS

	Aluminium Calorimeter	Graphite Calorimeter
Type	Quasi-adiabatic	Quasi-adiabatic
Material	Aluminium alloy	Graphite type EY927
Composition	94.5% Al, 5.2% Cu, 0.3% Fe + minor impurities.	100% C + minor impurities.
Density (kg m^{-3})	2.83×10^3	1.78×10^3
Specific heat ($\text{J kg}^{-1} \text{K}^{-1}$) at 28°C	875	730
Thermal conductivity ($\text{Wm}^{-1} \text{K}^{-1}$)	165	147 with grain 134 across grain
Absorber diameter (mm)	25.4	20.0
Absorber thickness (mm)	9.56	3.00
Absorber mass (g)	13.56	1.65
Absorber thermal leakage modulus (s^{-1})	1×10^{-4}	1×10^{-3}
Number of jackets	2 + vacuum chamber	3 + vacuum chamber
Vacuum gaps (mm)	1.6	0.25
Minimum depth, d (mm)	20.86	5.00
Vacuum chamber		
Window thickness (mm)	6.74 (Al)	0.05 (Melinex)
Maximum field size (mm)	90 dia or 70 x 70	100 dia or 80 x 80 (with provision for later extension to 200 mm x 200 mm).

TABLE 2
THE IRRADIATION CELL - USEFUL RANGE OF IRRADIATION CONDITIONS

z (m) Minimum Maximum	Horizontal Beam		Vertical Beam	
	0.48	3.0	0.48	2.0
Field (mm)				
Minimum	26 x 26	160 x 160	26 x 26	110 x 110
Maximum	200 x 200	1000 x 1000	200 x 200	650 x 650
Exposure: $\frac{\Delta X(x)}{\Delta t}$				
^{137}Cs (R min ⁻¹) (1.4 kCi)	23	0.6	23	1.4
^{60}Co (R min ⁻¹) (3.4 kCi)	270	7.0	270	16
Height (beam axis to floor)				
maximum (m)	2.0	1.5		
minimum (m)	0.76	0.89		
Timing accuracy	± 10%	± 1%		± 0.1%
Δt (Minimum)	3 sec	30 sec		300 sec

TABLE 3
THE ALUMINIUM CALORIMETER - CHARACTERISTICS

Bridge Supply Voltage Null Detector Range *	18V 1μV	
Recorder full scale (mm)	280	
Recorder full scale (μV)	2	
Thermistor temperature coefficient (% °C ⁻¹)	3.1	
Sensitivity (°C mm ⁻¹)	5 x 10 ⁻⁶	
Sensitivity (J mm ⁻¹)	6 x 10 ⁻⁵	
Sensitivity (rad mm ⁻¹)	0.44	
	Bridge Only	Overall
Peak to peak noise (μV)	3 x 10 ⁻²	3.3 x 10 ⁻²
Peak to peak noise, temperature equivalent (°C)	2 x 10 ⁻⁵	2.2 x 10 ⁻⁵
Average drift (μV min ⁻¹)	3 x 10 ⁻⁴	6 x 10 ⁻⁴
Average drift, temperature equivalent (°Cmin ⁻¹)	2 x 10 ⁻⁷	4 x 10 ⁻⁷

* The minimum range compatible with the bridge resistance is 0.3 μV.
Other ranges available are 3, 10, 30 μV etc. up to 100 mV.

TABLE 4

¹³⁷Cs SOURCE. MEASURED VALUES OF CURRENT, I(x), AND EXPOSURE, X(x), USING
THE GRAPHITE CAVITY CHAMBER

Column No.	2	3	4	5
Field = 47 x 47 mm t _o = 6/11/72	x = 677.2 mm d = 4.03 mm + d _w			
Wall Thickness (d _w)		I(x,d) (pA)	k _w	I(x) (pA) = k _w .I(x,d)
(mm)	(g cm ⁻²)			
1.154	0.1590	58.065	1.00925	58.603
2.148	0.2948	57.828	1.01341	58.603
3.178	0.4358	57.536	1.01990	58.680
5.246	0.7200	56.829	1.03321	58.717
6.178	0.8480	56.646	1.03928	58.871
9.276	1.2732	55.436	1.05984	58.753
12.327	1.6918	54.277	1.08066	58.655
16.357	2.2450	52.861	1.10910	58.628
22.602	3.1021	50.751	1.15531	58.634

Mean value of I(x) for d_w > 1.5 g cm⁻², $\bar{I}(x) = 58.639$.

$$\frac{\Delta X(x)}{\Delta t} = \frac{\bar{I}(x) \cdot \bar{S}_m \cdot k_1 \cdot k_2}{v \cdot \rho_o} = 5.033 \times 10^{-5} \text{ C kg}^{-1} \text{ s}^{-1}$$

TABLE 5

^{60}Co SOURCE. MEASURED VALUES OF CURRENT, $I(x)$, AND EXPOSURE, $X(x)$, USING THE GRAPHITE CAVITY CHAMBER

Column No.	2	3	4	5
Field = 47 x 47 mm $t_o = 6/11/72$	$x = 675.2 \text{ mm}$ $d = 4.03 \text{ mm} + d_w$			
Wall Thickness (d_w)	$I(x, d)$ (pA)	k_w	$I(x)$ (pA) $= k_w \cdot I(x, d)$	
(mm)				
1.154	0.1590	559.02	1.24146	694.00
2.148	0.2948	657.39	1.06004	696.86
3.1752	0.4358	678.16	1.02785	697.05
5.246	0.7200	673.10	1.02896	692.60
6.1784	0.8480	670.35	1.03370	692.94
9.276	1.2732	660.05	1.05089	693.65
12.327	1.6918	650.56	1.06829	694.99
12.327	1.6918	649.25	1.06829	693.59
16.357	2.2450	635.80	1.09182	694.17
22.602	3.1021	619.35	1.12948	699.54
36.811	5.0523	568.37	1.22104	693.99

Mean value of $I(x)$ for $d_w > 1.5 \text{ g cm}^{-2}$, $\bar{I}(x) = 695.26$.

$$\frac{\Delta X(x)}{\Delta t} = \frac{\bar{I}(x) \cdot \bar{S}_m \cdot k_1 \cdot k_2}{v \cdot \rho_o} = 5.920 \times 10^{-4} \text{ C kg}^{-1} \text{ s}^{-1}$$

TABLE 6

MEASURED CURRENT, $I_t(x)$, FOR BALDWIN-FARMER CHAMBER (No. 617030)

Radiation Quality	$I_t(x)$ (pA)	
	$x = 677.2 \text{ mm}, t_o = 6/11/72, \text{Field} = 47 \times 47 \text{ mm}$	
	Perspex Cap	Aluminium Cap
^{137}Cs	34.117	34.551
^{60}Co	409.21	421.21

TABLE 7

EXPOSURE CALIBRATION FACTOR, N, FOR BALDWIN-FARMER CHAMBER (No. 617030)

Cavity Chamber-Thimble Chamber Inter Comparison (Tables 4, 5, 6)					
$N = \frac{\Delta X(x)}{\Delta t} \cdot \frac{1}{2.58 \times 10^{-4} \bar{I}_t(x) \cdot k_1 \cdot k_2 \cdot k_{32}}$					
Calorimeter-Thimble Chamber Inter Comparison (Tables 8 and 9)					
$N = \frac{\Delta D(x,d) \cdot k_d \cdot (\mu_{en}/\rho)_{air} \cdot k_1 \cdot k_2 \cdot k_{10} \cdot k_{11} \cdot k_{12}}{\Delta_t \cdot \bar{W} \cdot (\mu_{en}/\rho)_{Al} \cdot 2.58 \times 10^{-4} \cdot \bar{I}_t(x,d) \cdot k_1 \cdot k_2 \cdot k_{33} \cdot k_{34}}$					
1	2	3	4	5	6
Radiation Source	Effective Energy (MeV)	Calibration Factor, N (GR C ⁻¹)*			
		Perspex Cap		Aluminium Cap	
		By AAEC Graphite Chamber	By NPL	By AAEC Graphite Chamber	By AAEC Aluminium Calorimeter
¹³⁷ Cs (degraded)	0.58 + 0.04 - 0.07	-	-	-	5.75 ± 0.23
¹³⁷ Cs	0.62 ± 0.04	5.72 ± 0.24	-	5.65 ± 0.24	- -
2MV X-ray (mm Cu HVL)	0.8 ± 0.05	-	5.46 ± ?	-	-
⁶⁰ Co (degraded)	1.08 + 0.04 - 0.07	-	-	-	5.37 + 0.18 - 0.25
⁶⁰ Co	1.16 ± 0.04	5.57 ± 0.23	-	5.42 ± 0.23	-

* 1 GR = 10⁹ roentgen

TABLE 8

¹³⁷Cs SOURCE. MEASURED VALUES OF DOSE, D (x,d), AND THIMBLE
CHAMBER CURRENT, I_t (x,d), IN ALUMINIUM

1	2	3	4	5	6	7	
Date	Time	Field = 68 x 68 mm, t ₀ = 6/11/72					
		x = 570.2 mm, d = 27.60 mm					x = 570.0 mm d = 27.78 mm
		Radiation $\Delta T(x,d)/\Delta t$ (mm s ⁻¹)	Elec.Heating $\Delta E/\Delta T$ (J m ⁻¹)	Drift (%)	Δt (min)		I _t (x,d) (pA)
6/10/72	1010		0.171613	+ 0.58	13.043	43.6429	
	1100	0.158761		+ 1.79	23.945		
	1200		0.173125	+ 1.21	13.178		
	1230	0.156542		+ 1.99	24.212		
	1400		0.171416	+ 1.40	13.025		
	1430	0.158486		+ 2.35	24.005		
	1520		0.174457	+ 0.78	13.173		
	1602						
7/10/72	1000		0.171949	+ 0.02	11.360	43.4779	
	1030	0.159037		+ 1.51	25.950		
	1115		0.171235	+ 1.16	12.543		
	1200	0.159194		+ 2.32	25.718		
	1315		0.171845	+ 0.97	12.593		
	1400	0.162377		+ 1.99	25.248		
	1500		0.171004	+ 0.98	12.937		
	1540						
9/10/72	1053					43.4912	
	1130		0.172041	+ 0.83	12.457		
	1210	0.161132		+ 2.02	24.920		
	1400	0.158384		+ 0.72	24.930		
	1430		0.173298	+ 0.75	12.423		
	1520	0.160965		+ 2.84	25.125		
	1620		0.170176	+ 1.58	12.373		
10/10/72	1100	0.158425		+ 0.13	24.039	43.3971	
	1200		0.174346	+ 0.09	12.825		
	1230	0.158295		+ 0.41	25.370		
	1400		0.171471	+ 0.19	12.108		
	1435	0.158050		+ 0.99	25.050		
	1615						

Mean 0.159137 0.172152 $\bar{I}_t(x,d) = 43.5022$
 σ (%) 1.0 0.75 0.23
 $\bar{\sigma}$ (%) 0.29 0.21 0.11

$$\frac{\Delta D(x,d)}{\Delta t} = \frac{\Delta T(x,d)}{\Delta t} \cdot \frac{\Delta E}{\Delta T} \cdot \frac{1}{m} = 2.0224 \text{ mJ kg}^{-1} \text{ s}^{-1}$$

TABLE 9

^{60}Co SOURCE, MEASURED VALUES OF DOSE, $D(x,d)$, AND THIMBLE
CHAMBER CURRENT, $I_t(x,d)$, IN ALUMINIUM

1	2	3	4	5	6	7	
Date	Time	Field = 68 x 68 mm, $t_o = 6/11/72$					$I_t(x,d)$ (pA)
		x = 571.2 mm, d = 27.60 mm				x = 571.1 mm d = 27.78 mm	
		Radiation $\Delta T(x,d)/\Delta T$ (mm s ⁻¹)	Elec. Heating $\Delta E/\Delta T$ (J m ⁻¹)	Drift (%)	Δt (min)		
24/10/72	1230		0.574405	- 0.33	6.930	551.256	
	1245	0.574216		0	7.148		
	1405		0.573637	- 0.02	7.138		
	1440	0.568256		- 0.10	7.232		
	1500		0.573498	+ 0.25	7.348		
	1520	0.571066		+ 0.57	7.402		
	1550		0.574654	+ 0.64	7.343		
	1615						
25/10/72	1346					551.431	
	1415		0.572888	+ 0.29	7.157		
	1440	0.571803		+ 0.39	7.217		
	1500		0.574842	+ 0.64	7.308		
	1540		0.576927	+ 0.77	6.207		
	1600	0.574280		+ 1.3	7.411		
	1630		0.576794	+ 0.79	6.445		
26/10/72	0945	0.571895		+ 0.12	7.150	551.968	
	1200		0.575499	+ 0.13	6.488		
	1225	0.570511		+ 0.37	7.251		
	1250		0.575813	+ 0.51	6.503		
	1415	0.572396		+ 0.55	7.298		
	1430		0.577737	+ 0.31	6.522		
	1450	0.567829		+ 0.39	7.320		
	1520		0.576346	+ 0.64	6.575		
1620							

Mean	0.571361	0.575253	$I_t(x,d) = 551.552$
σ (%)	0.40	0.26	0.067
$\bar{\sigma}$ (%)	0.13	0.076	0.039

$$\frac{\Delta D(x,d)}{\Delta t} = \frac{\Delta \bar{T}(x,d)}{\Delta t} \cdot \frac{\Delta \bar{E}}{\Delta T} \cdot \frac{1}{m} = 24.264 \text{ mJ kg}^{-1} \text{ s}^{-1}$$

TABLE 10

ACCURACY OF IONIMETRIC CALIBRATION OF THE THIMBLE CHAMBER

Source of Error	Error (99% Confidence Level)		
	Random (%)	Systematic (%)	Total (%)
A. <u>Measurement of Exposure</u>			
$I(x,d)$.	0.2	0.1	
v .		0.5	
\bar{S}_m (ICRU 1962) .		2.0	
k_w .	0.5	0.5	
$k_o, k_1, k_2, k_{20}, k_{21}$.	0.2	0.1	
Total	0.6	3.2	3.8
B. <u>Measurement of Thimble Chamber Current</u>			
$I_t(x)$.	0.2	0.1	
$k_o, k_1, k_2, k_{30}, k_{31}, k_{32}$.	0.2	0.2	
Total	0.2	0.3	0.5
Calibration Factor, N. (A + B)	0.7	3.5	4.2

TABLE 11

ACCURACY OF CALORIMETRIC CALIBRATION OF THE THIMBLE CHAMBER

Source of Error		Error (99% Confidence Level)		
		Random (%)	Systematic (%)	Total (%)
A. <u>Measurement of Absorbed Dose</u>				
$\Delta\bar{T}$ (x,d):	¹³⁷ Cs	0.9		
	⁶⁰ Co	0.4		
Δt :	⁶⁰ Co	0.1		
$\frac{\Delta\bar{E}}{\Delta\bar{T}}$:	¹³⁷ Cs	0.5		
	⁶⁰ Co	0.2		
m:			0.3	
$k_0, k_1, k_2, k_{10}, k_{11}, k_{12}$:			0.4	
Total:	¹³⁷ Cs	1.0	0.7	1.7
	⁶⁰ Co	0.5	0.7	1.2
B. <u>Conversion of Absorbed Dose to Exposure in a Finite Cavity</u>				
\bar{W} :			1.0	
$(\mu_{en}/\rho)_{air}/(\mu_{en}/\rho)_{Al}$:	¹³⁷ Cs		0.5	
	⁶⁰ Co		+0.5, -1.7	
k_d :	¹³⁷ Cs		0.7	
	⁶⁰ Co		0.5	
Total:	¹³⁷ Cs		2.2	2.2
	⁶⁰ Co		+2.0, -3.2	+2.0, -3.2
C. <u>Measurement of Thimble Chamber Current</u>				
I_t (x,d):		0.2	0.1	
$k_0, k_1, k_2, k_{33}, k_{34}$:		0.1		
Total:		0.3	0.1	0.4
Calibration Factor, N:	¹³⁷ Cs	1.0	3.0	4.0
	⁶⁰ Co	0.6	+2.8, -4.0	+3.4, -4.6

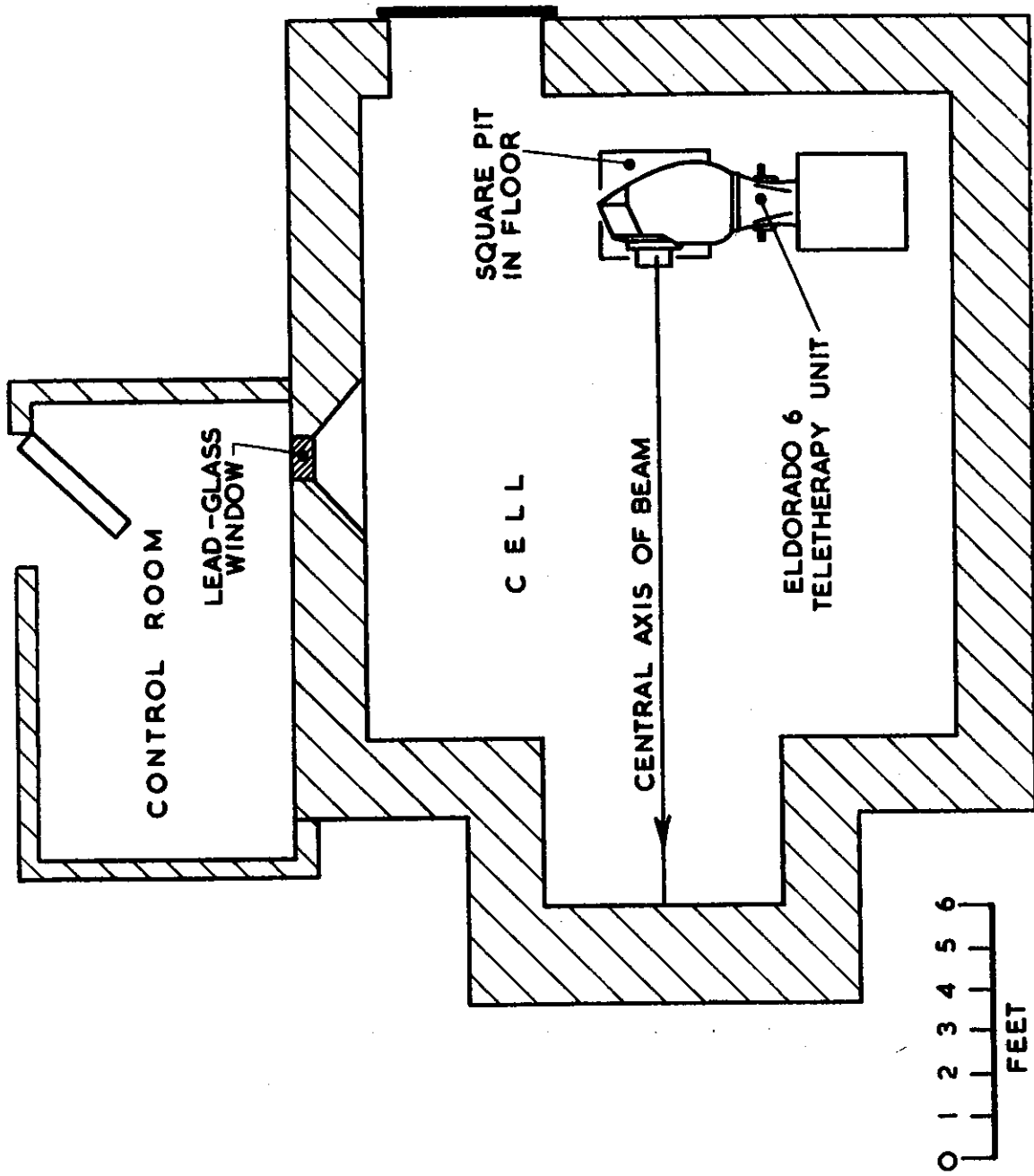


FIGURE 1. PLAN OF IRRADIATION CELL

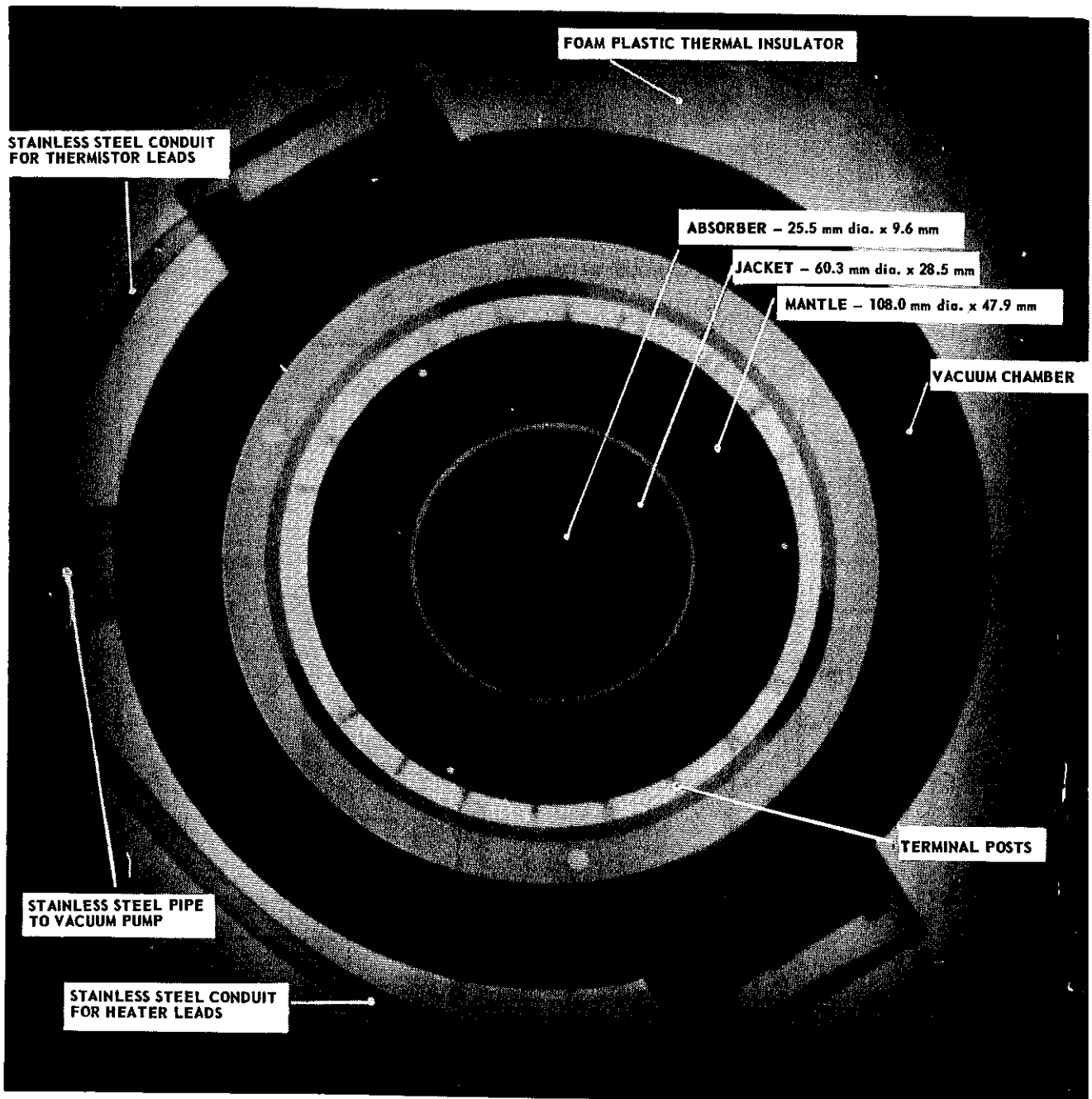


FIGURE 2. RADIOGRAPH OF ALUMINIUM CALORIMETER

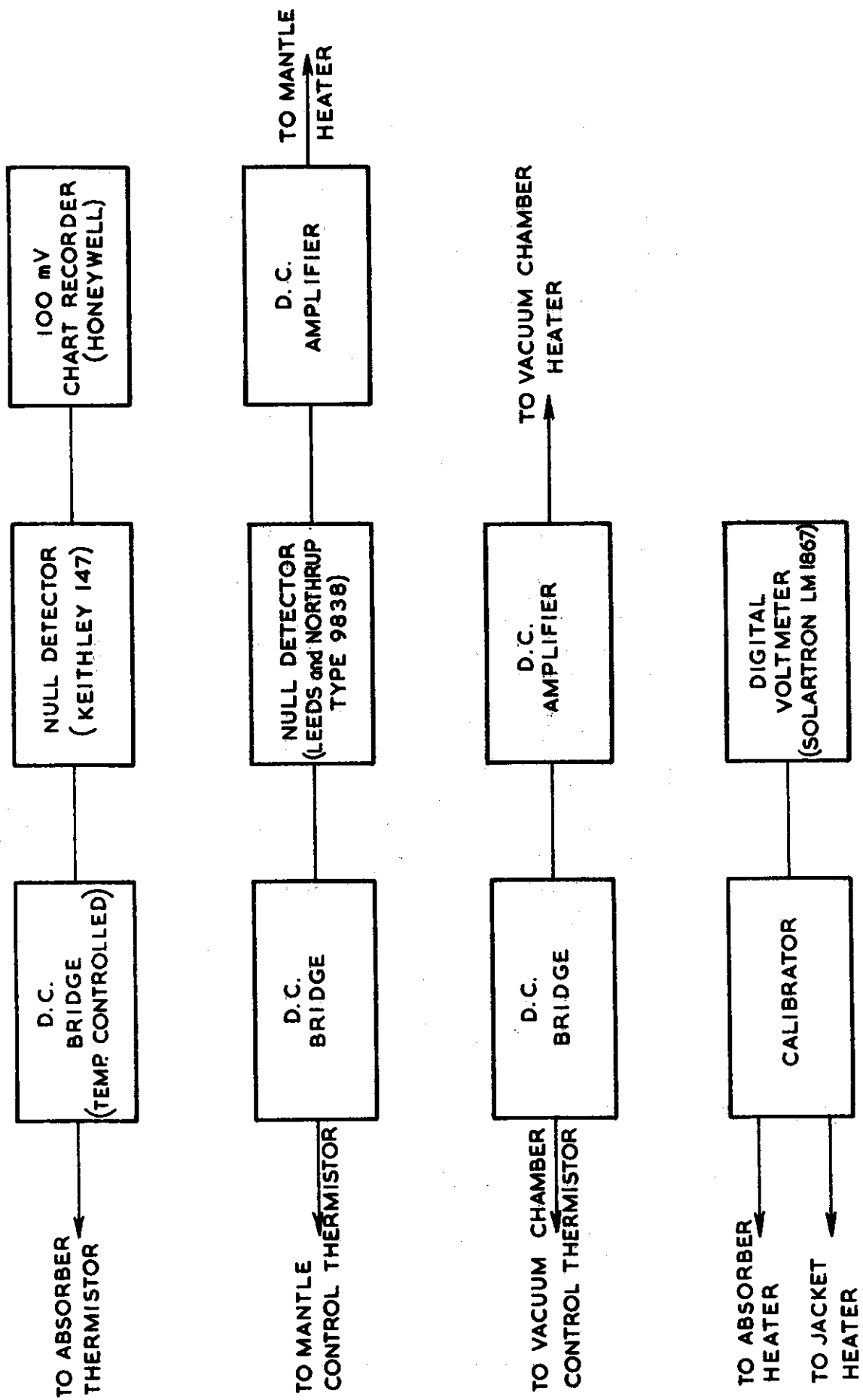


FIGURE 3. BLOCK DIAGRAM OF CALORIMETER TEMPERATURE MEASUREMENT AND CONTROL SYSTEM

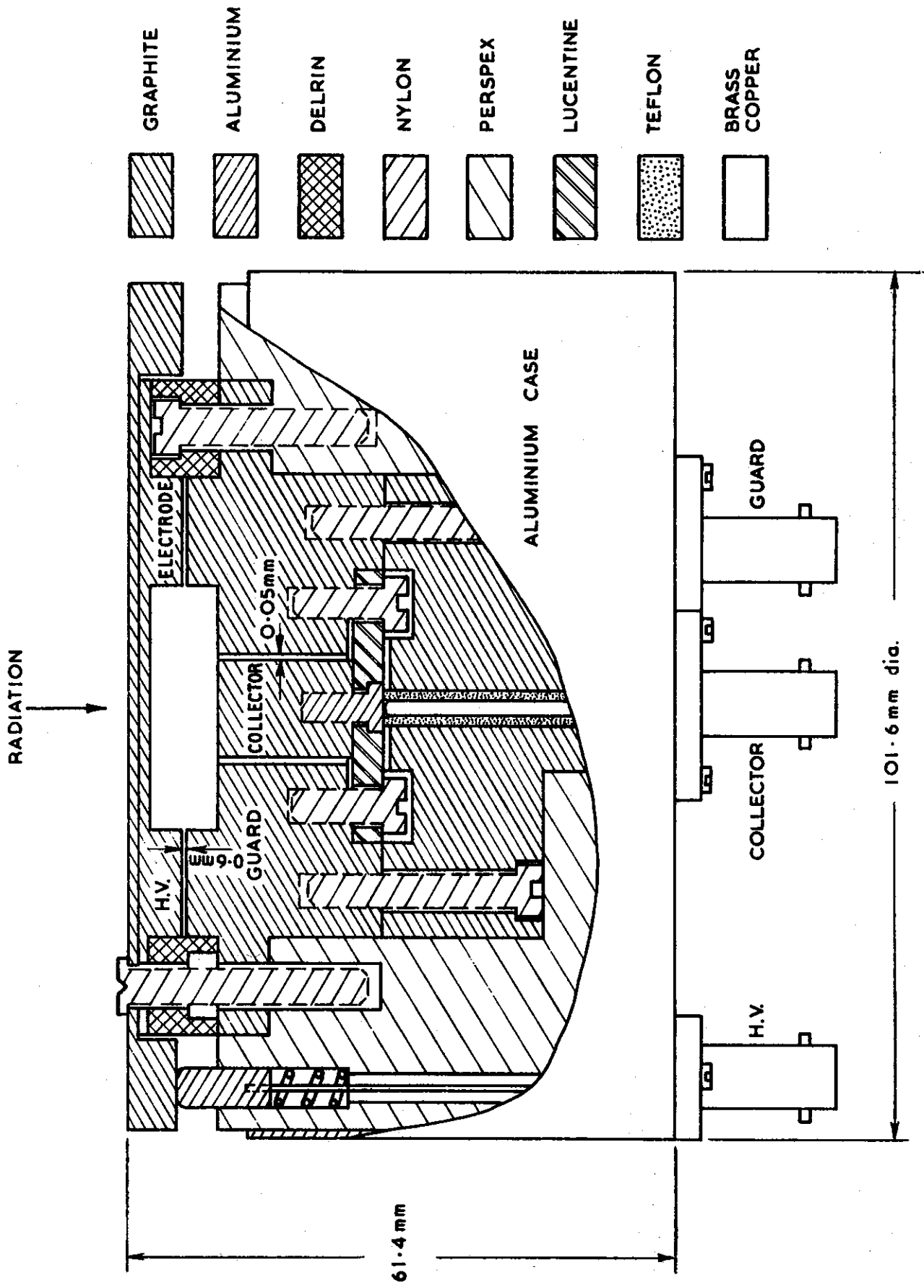


FIGURE 4. GRAPHITE CAVITY CHAMBER

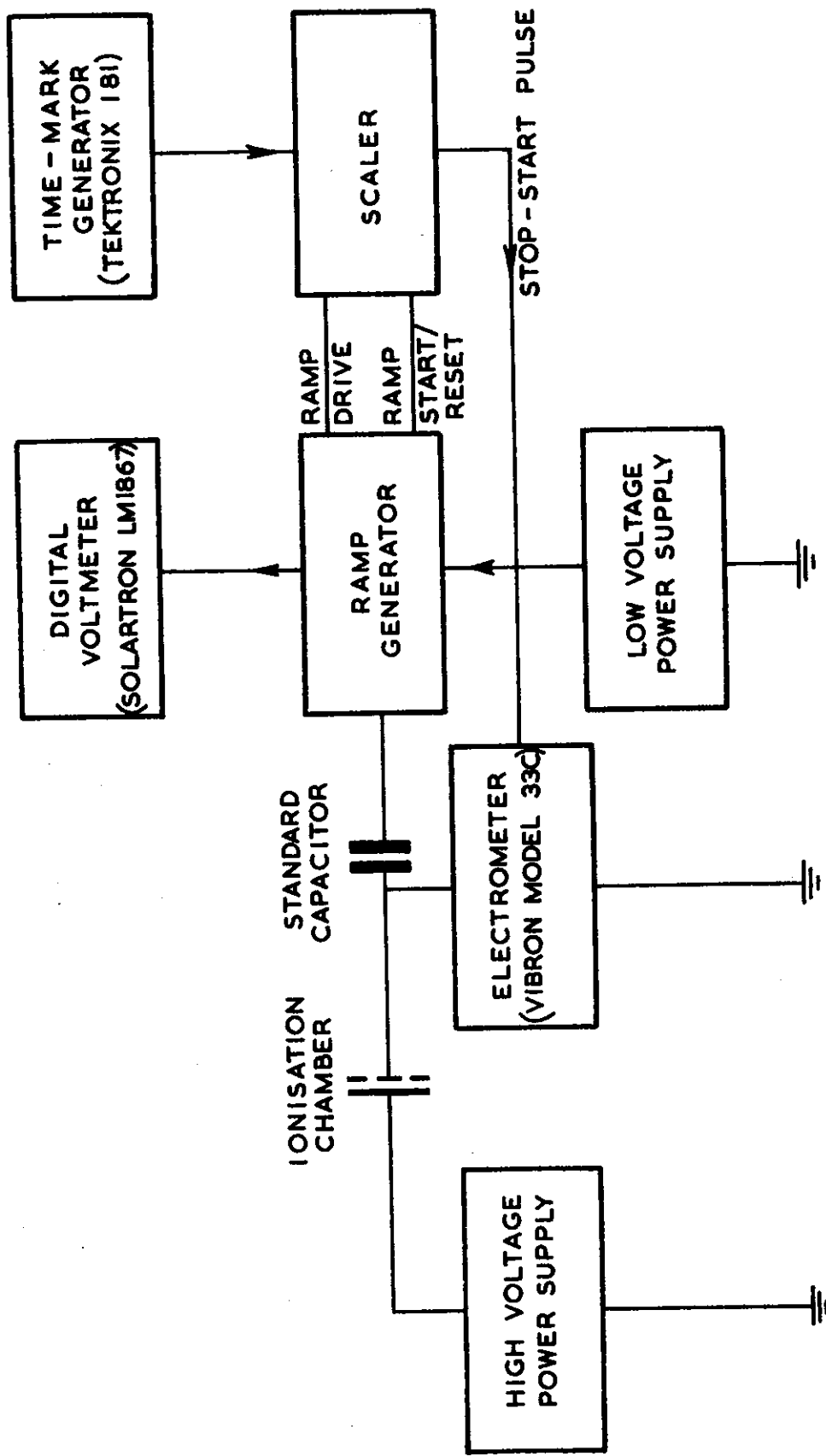


FIGURE 5. BLOCK DIAGRAM OF TOWNSEND BALANCE

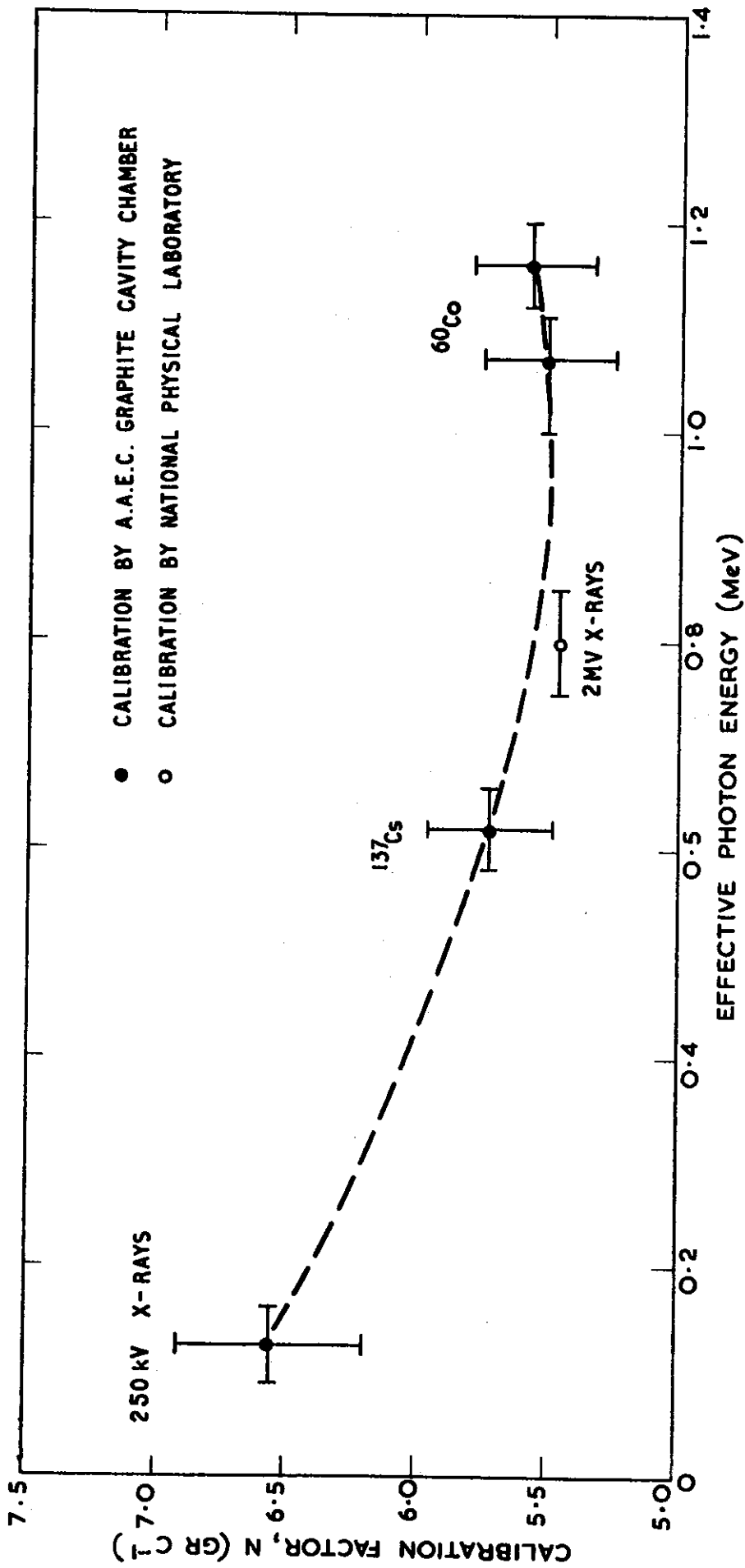


FIGURE 6. ENERGY RESPONSE OF THE BALDWIN-FARMER CHAMBER WITH THE PERSPEX CAP

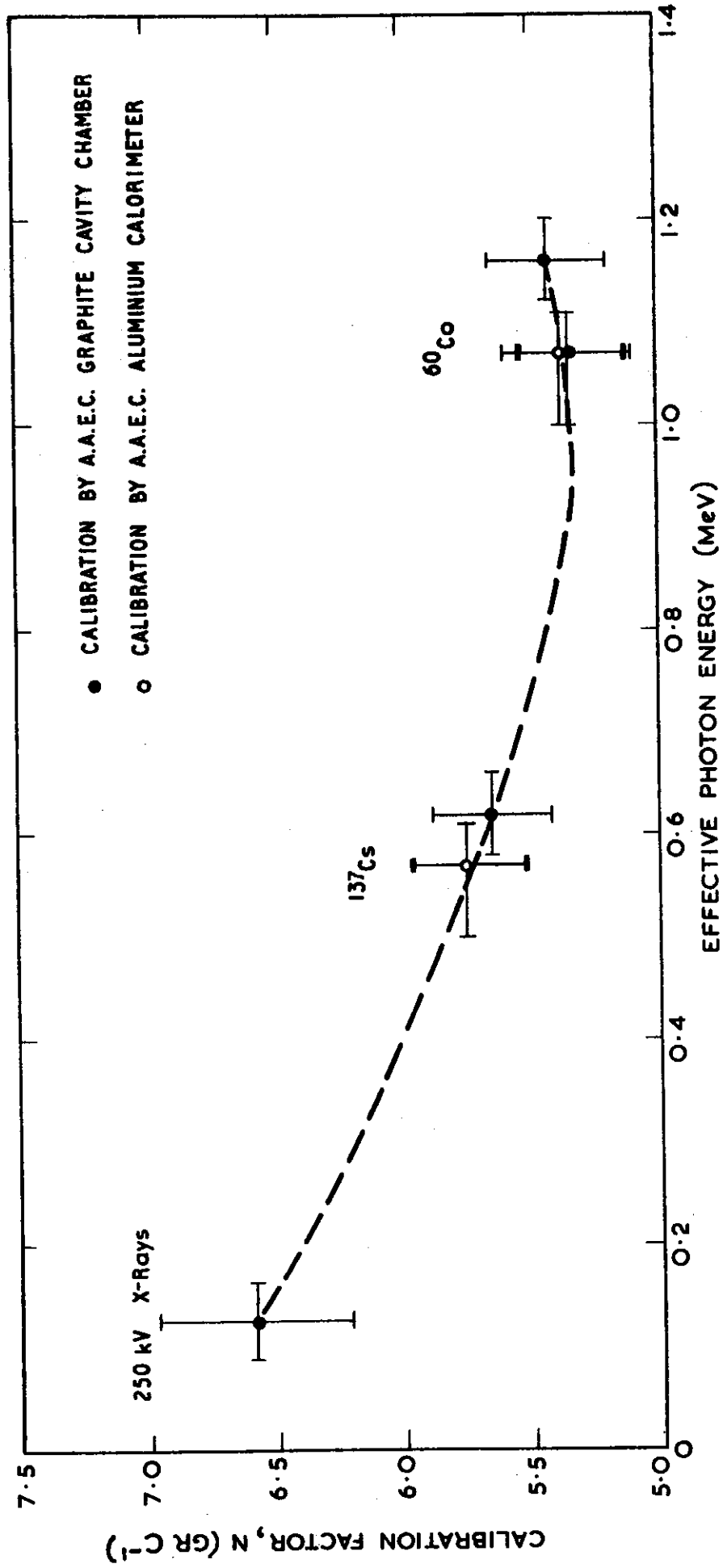


FIGURE 7. ENERGY RESPONSE OF THE BALDWIN-FARMER CHAMBER WITH THE ALUMINIUM CAP

APPENDIX A
DEFINITION OF SYMBOLS AND TERMS

A1 TERMS

Cavity. The sensitive volumes of dosimeters in general, such as the collecting volume of a cavity chamber or the absorber element of the calorimeter.

A very small cavity. The smallest possible cavity consistent with the ICRU definitions of exposure and absorbed dose, ICRU (1968). In the present context this generally means less than 1 mm^3 .

Aluminium. Any reference to aluminium refers to the particular alloy used for the calorimeter; this alloy contains about 5% copper.

Accuracy. This term refers to absolute accuracy and any figures quoted are for the 99% confidence level.

A2 SYMBOLS

- x. The distance along the central axis of the beam from the source face to the centre of a cavity.
- d. The depth to the centre of a cavity in a solid medium. This distance does not include vacuum or air gaps between the cavity and the surface of the medium.
- d_w . The effective front wall thickness of a cavity chamber.
- r. The radius or half-thickness of a cavity measured along the central beam axis.
- X(x). The exposure in air at distance x.
- X(x,d). The exposure in a very small air cavity at distance x and depth d in a solid medium.
- X(x,d,r). The exposure in a finite air cavity of radius or half-thickness r at depth d and distance x.
- D(x,d). The absorbed dose in a very small cavity at distance x and depth d.
- $\Delta X(x)/\Delta t$. The exposure rate in air. Other exposure and dose rates are shown in the same way.
- I(x,d). The ionisation current (at distance x and depth d) in a cavity chamber filled with dry air at 0°C and 760 mm Hg.
- I(x). The ionisation current in an ideal cavity chamber in which there is full electronic equilibrium and zero photon attenuation in the front wall.
- $I_t(x)$. The ionisation current in a thimble transfer chamber (22°C and

- 760 mm Hg) at distance x , in air.
- $I_t(x,d)$. The ionisation current in a thimble chamber (22°C and 760 mm Hg) at distance x , and at depth d , in a solid medium.
- v . Cavity volume.
- m . Cavity mass.
- ρ . Density of cavity wall material.
- ρ_0 . Density of air at 0°C and 760 mm Hg.
- μ . Linear attenuation coefficient for photons.
- β . Linear attenuation coefficient for secondary electrons.
- a . Linear photon scattering coefficient.
- μ_{en} . Linear energy absorption coefficient.
- \bar{S}_m . Mean mass stopping power ratio (relative to air).
- Δt . Duration of an exposure.
- N . Exposure calibration factor for a transfer thimble chamber in units of roentgen per coulomb.
- \bar{W} . Average energy required to produce an ion pair in air.
- σ . Standard deviation for a single measurement in a set of measurements.
- $\bar{\sigma}$. Standard deviation of the mean value of a set of measurements.
- $h\nu_0$. Photon energy in a monoenergetic beam.
- $h\bar{\nu}$. Mean photon energy in a composite spectrum.
- $h\nu(\theta)$. Energy of a photon after being scattered through an angle θ .
- $\sigma(\theta)$. Klein - Nishina cross section for photon scattering through the angle, θ .
- k_0 etc. Symbols for the correction factors are defined in Appendix B.

APPENDIX B

EVALUATION OF THE CORRECTION FACTORS, COEFFICIENTS AND CONSTANTS

B1 CORRECTION FACTORS RELATING TO THE IRRADIATION FACILITY

k_o

$$k_o = Z_o/Z_r = \exp(0.693147 t/T_{1/2}),$$

where

Z_r = the exposure or dose at time t_r ,

Z_o = the exposure or dose at time t_o (an arbitrary reference time),

$T_{1/2}$ = the half-life of the radioisotope source

$$= \begin{cases} 30.0 \text{ years for } ^{137}\text{Cs} \\ 1922 \text{ days for } ^{60}\text{Co, and} \end{cases}$$

$$t = t_r - t_o$$

This correction is included in all 'observed' values shown in this report; the errors involved are negligible.

k_1

A k_1 correction should be made, in principle, for random fluctuations in the output of the teletherapy unit, which could be produced by small changes in the source position with respect to the collimator. Although a beam monitor was not used for the reported measurements, it was found that, by taking repeated measurements of the exposure at a fixed point in the beam and operating the source On/Off mechanism between each measurement, the output of the unit was stable to better than $\pm 0.1\%$. In this report the value $k_1 = 1.0 \pm 0.1\%$ is used.

k_2

A k_2 correction could also be made for nonuniformity of beam intensity in directions at right angles to the beam axis. Since all comparative measurements were made with the same field size, using instruments in which the cross sectional areas of the sensitive elements were approximately equal and small compared with the field area, this correction was not applied. The error involved was estimated conservatively at 0.1% , e.g. $k_1 = 1.0 \pm 0.1\%$.

B2 CORRECTION FACTORS APPLIED TO THE CALORIMETER MEASUREMENTS

k_{10}

$$k_{10} = Z_a/Z_t = R_a/(R_a + R_l) = 0.9969 \pm 0.03\%,$$

where

Z_t = the measured total electric power delivered to the

calorimeter during calibration (including power dissipated in the leads to the heater),

Z_a = power delivered to the absorber heater during calibration,

R_a = the resistance of the absorber heater (767.0 Ω), and

R_l = the lead resistance (2.4 Ω)

k_{11}

$$k_{11} = Z_c / \bar{Z}$$

where

Z_c = the absorbed dose at the centre of the calorimeter absorber, and

\bar{Z} = the mean absorbed dose averaged over the extent of the absorber (as measured by the calorimeter).

This correction was evaluated mathematically assuming an inverse square law for the beam divergence and an exponential law for the attenuation of the beam across the thickness of the absorber. It was found that:

$$k_{11} = 2\mu r \left(1 - \frac{r^2}{x^2}\right) \exp(\mu r) / (\exp(2\mu r) - 1)$$

$$= \begin{cases} 0.9983 \pm 0.02\% \text{ for } ^{137}\text{Cs} \\ 0.9990 \pm 0.02\% \text{ for } ^{60}\text{Co} \end{cases}$$

where

x = the distance from the source to the centre of the absorber (570.2 mm)

r = the half-thickness of the absorber (4.78 mm), and

μ = the linear attenuation coefficient

$$= \begin{cases} 20.9 \text{ (m}^{-1}\text{) for } ^{137}\text{Cs} \\ 15.1 \text{ (m}^{-1}\text{) for } ^{60}\text{Co} \end{cases}$$

k_{12}

$$k_{12} = Z/Z^1$$

$$= \frac{\mu_{en}}{\mu^1_{en}} \cdot \frac{[\exp(-\mu d) (1 + \sin a d)]}{[\exp(-\mu^1 d) (1 + \sin a^1 d)]}$$

$$= \begin{cases} 0.9953 \pm 0.3\% \text{ for } ^{137}\text{Cs} \\ 0.9962 \pm 0.3\% \text{ for } ^{60}\text{Co} \end{cases}$$

where

Z = the absorbed dose in an ideal aluminium calorimeter free from foreign components such as heater wires, epoxy cement, thermistors and vacuum pumping ducts.

Z^1 = the absorbed dose in the actual calorimeter,
 d = the depth to the centre of the absorber (27.6 mm),
 μ_{en} , μ , 'a' are linear energy absorption, attenuation and scattering coefficients for the ideal calorimeter, and μ_{en}^1 etc. the coefficients for the actual calorimeter.

The values of these coefficients used for calculating k_{12} are shown in Table B1.

TABLE B1
THE VALUE OF COEFFICIENTS USED TO CALCULATE k_{12}

Source	μ_{en} (m^{-1})	μ_{en}^1 (m^{-1})	μ (m^{-1})	μ^1 (m^{-1})	a (m^{-1})	a^1 (m^{-1})
^{137}Cs	8.046	7.940	21.06	20.79	14.43	14.23
^{60}Co	7.281	7.187	15.26	15.07	8.83	8.71

These coefficients were evaluated on the basis of an absorber composition for the ideal calorimeter of 94.5% Al, 5.2% Cu, 0.3% Fe and for the actual calorimeter, 93.3% Al, 5.3% Cu, 0.3% Fe and 1.1% epoxy (75% C, 6% H and 19% O). The mean density over the depth, d , was $2.83 \times 10^3 \text{ kg m}^{-3}$ for the ideal calorimeter and $2.79 \times 10^3 \text{ kg m}^{-3}$ for the actual calorimeter. The experimental determination of the scatter coefficient, 'a', for aluminium is described in Section B5.

B3 CORRECTION FACTORS APPLIED TO THE GRAPHITE CAVITY CHAMBER

k_{20}

$$k_{20} = \frac{(T + 273.15)}{273.15} \cdot \frac{760}{p}$$

where

T = air temperature ($^{\circ}\text{C}$) at the time of measurement, and

p = air pressure (mm Hg) at the time of measurement.

This correction is included in all the 'observed' values of measurements shown in this report. The maximum error involved is less than 0.1%.

No correction was made for humidity, in accordance with the findings of Loftus et al. (1966).

k_{21}

All the observed values of ion current shown here include a correction for lack of saturation. The k_{21} correction factor was evaluated graphically by plotting the current I against I/V_c^2 , and extrapolating to the $I/V_c^2=0$ axis

(Greening 1964). V_c is the polarising potential applied to the chamber. The value for k_{21} is $1.0 + 0.02\%$.

B4 CORRECTION FACTORS APPLIED TO THE THIMBLE CHAMBER MEASUREMENTS

k_{30}

$$k_{30} = \frac{(T + 273.15)}{(22 + 273.15)} \cdot \frac{760}{p}$$

where $T(^{\circ}\text{C})$ and p (mm Hg) were the air temperature and pressure at the time of measurement. This correction is included in all 'observed' values and the errors involved are less than 0.05%.

k_{31}

k_{31} corrects for lack of saturation in the thimble chamber, and is included in the measured values given in this report. The value of this correction is $1.0 \pm 0.1\%$.

k_{32}

k_{32} is a small inverse square law correction for small differences in the distance x , from the source to the thimble and cavity chambers during intercomparison.

$$k_{32} = \begin{cases} 1.0000 \pm 0.05\% \text{ for } ^{137}\text{Cs} \\ 1.0059 \pm 0.05\% \text{ for } ^{60}\text{Co} \end{cases}$$

k_{33}

The k_{33} correction factor is similar to k_{32} but applies to thimble chamber calorimeter intercomparisons.

$$k_{33} = \begin{cases} 0.9993 \pm 0.05\% \text{ for } ^{137}\text{Cs} \\ 0.9996 \pm 0.05\% \text{ for } ^{60}\text{Co} \end{cases}$$

k_{34}

k_{34} is an attenuation correction for small differences in the depth, d , of the calorimeter absorber and the cavity in the dummy calorimeter for the thimble chamber.

$$k_{34} = \begin{cases} 1.0021 \pm 0.05\% \text{ for } ^{137}\text{Cs} \\ 1.0015 \pm 0.05\% \text{ for } ^{60}\text{Co} \end{cases}$$

B5 DISPLACEMENT FACTOR, COEFFICIENTS AND CONSTANTS

Displacement Factor (k_d)

The displacement factor, k_d , defined by Equation (5) (see Section 8) was calculated from the equation:

$$k_d = \frac{\exp(-\mu \bar{d}_w) (1 + \sin(a \cdot \bar{d}_w))}{\exp(-\mu d) (1 + \sin(a \cdot d))} = \begin{cases} 1.0506 \pm 0.7\% \text{ for } ^{137}\text{Cs} \\ 1.0371 \pm 0.5\% \text{ for } ^{60}\text{Co} \end{cases}$$

where

\bar{d}_w = the effective front wall thickness for a cylindrical cavity
with its centre at depth d , and

μ = linear attenuation }
 a = scatter } coefficient for aluminium

The effective front wall thickness was estimated by averaging over the curved surface of the cavity (radius r):

$$\bar{d}_w = d - \frac{r}{2} \int_{-\pi/2}^{\pi/2} \cos^2 \theta d\theta ,$$

$$= d - \frac{\pi r}{4} = d - 0.79 r .$$

Coefficients a and β for Graphite and Aluminium

Although the theoretical expression for cavity chamber wall corrections developed by Barnard et al. (1959) was applied to cylindrical chambers, their treatment of the problem was developed from consideration of a cavity with a flat front wall; a correction for wall curvature in cylindrical chambers was incorporated later. It therefore seems valid to apply the same basic expression (without the wall curvature correction) to the graphite parallel plate chamber used here. In its simplest form the correction of Barnard et al. (1962) can be written

$$I(x) = I(x,d) / [\exp(-\mu d_w) (1 + \sin a.d_w) - \exp(-\beta d_w)] \quad \dots(B1)$$

using symbols defined in Appendix A.

$I(x,d)$ was measured for 10 values of wall thickness over the range 0.2 to 5 g cm⁻². Using Equation B1, a value for $I(x)$ was derived for each experiment from which was calculated the standard deviation of $I(x)$. This calculation was repeated (using a programmed electronic desk calculator) for a range of values of a and β to search for coefficients which give a minimum standard deviation. In the case of ¹³⁷Cs, the wall thickness could not be made small enough to obtain a reliable measurement of β but the walls used for actual exposure measurements were so thick that the $\exp(-\beta.d_w)$ term in Equation (B1) was negligible.

The a coefficient for aluminium was measured in the same way, using a series of aluminium caps of increasing thickness made to fit the thimble chamber. All caps were thick enough to ensure electronic equilibrium in the aluminium and to make the β term in Equation (B1) very small. In this case a wall curvature correction was made following the method of Barnard et al. (1959). Values for a and β are shown in Table B2.

TABLE B2

VALUES OF THE COEFFICIENTS a AND β FOR ALUMINIUM
AND GRAPHITE USING ^{137}Cs AND ^{60}Co

	^{137}Cs	^{60}Co
a (graphite) (m^{-1})	4.400	2.365
a (Al) (m^{-1})	14.43	8.83
β (graphite) (m^{-1})	5360?	1444

Values of the scatter coefficient, a , determined for the graphite chamber are significantly lower than predicted by Equation (4) of Barnard et al. (1964). This is to be expected since the attenuation coefficients used were too low (see Section 9) and, consequently, low values of a were obtained when the wall attenuation equation was made to fit our experimental results. The wall attenuation corrections were recalculated using attenuation coefficients applicable to a ^{60}Co spectrum containing a 15% scatter component and a ^{137}Cs spectrum containing 20% of scattered radiation. The corrections obtained differed by less than 0.26% from those shown in Tables 4 and 5. This is considered to be the largest error which could be incurred in this way and has been included in the figures for over-all accuracy shown in Table 10.

Wall corrections (k_w), made using Equation (B1), were found to be generally 0.2 to 0.3% higher than corrections found by extrapolation of the linear part of the current against wall thickness curve to zero wall thickness.

μ_{en} , μ , \bar{S}_m and \bar{W}

The energy absorption and attenuation coefficients in Table B3 were calculated from tabulations by Evans (1968). The absorption coefficients for aluminium were calculated for an absorber composed of 93.3% Al, 5.3% Cu, 0.3% Fe and 1.1% epoxy.

The stopping power ratios and \bar{W} values were taken from the ICRU (1962).

TABLE B3
THE VALUES OF CONSTANTS USED IN CALCULATIONS

Coefficient	^{137}Cs	^{60}Co
$(\mu_{\text{en}}/\rho)_{\text{air}}$ ($\text{m}^2 \text{kg}^{-1}$)	$2.940 \times 10^{-3} \pm 0.2\%$	$2.656 \times 10^{-3} \pm 0.2\%$
$(\mu_{\text{en}}/\rho)_{\text{Al}}$ ($\text{m}^2 \text{kg}^{-1}$)	$2.843 \times 10^{-3} \pm 0.5\%$	$2.573 \times 10^{-3} \pm 1.5\%$ - 0.5%
μ_{graphite} (m^{-1})	$10.601 \pm 0.2\%$	$7.70 \pm 0.2\%$
\bar{S}_m (carbon/air)	$1.010 \pm 2\%$	$1.002 \pm 2\%$
\bar{W} (eV/ion pair or J C^{-1})	$33.7 \pm 1\%$	

APPENDIX C

THE MEAN ENERGY OF THE PHOTON SPECTRUM AT THE CALORIMETER ABSORBER

The mean energy ($\overline{h\nu}$) of the photon spectrum seen at the centre (P) of the calorimeter absorber will be lower than the incident photon energy ($h\nu_0$) due to scattering of the beam in traversing the depth, d , of aluminium. If the scatter coefficient, a , which has been measured experimentally for aluminium (Appendix B) is used as a measure of the contribution of scattered photons to the total spectrum at P, $\overline{h\nu}$ can be estimated from the following equation:

$$\overline{h\nu} = (\overline{h\nu})_s + \frac{h\nu_0 - (\overline{h\nu})_s}{1 + \sin ad} \quad \dots (C1)$$

where

$(\overline{h\nu})_s$ = the mean energy of scattered photons arriving at P.

The value of $(\overline{h\nu})_s$ can be found easily if the simplifying assumption is made that all scattering events in the beam occur in a plane normal to the beam at depth $d/2$. If a circular field of diameter, f , is considered, in which the field area is the same as for the square field used in the calorimeter measurements, then $(\overline{h\nu})_s$ is approximately

$$(\overline{h\nu})_s = \frac{\int_0^\phi \sin \theta \cdot \sigma(\theta) \cdot h\nu(\theta) \cdot d\theta}{\int_0^\phi \sin \theta \cdot \sigma(\theta) \cdot d\theta}$$

where

$$\phi = \tan^{-1} (f/d) ,$$

$h\nu(\theta)$ = the energy of photons scattered through an angle θ , and

$\sigma(\theta)$ = the Klein-Nishina cross section for scattering through the angle θ .

Using values of $h\nu(\theta)$ and $\sigma(\theta)$ published by Nelms (1953), this integral was evaluated numerically for the following results:

$$(\overline{h\nu})_s = \begin{cases} 0.50 \text{ MeV for } ^{137}\text{Cs} \\ 0.85 \text{ MeV for } ^{60}\text{Co} \end{cases}$$

Using these values in Equation C1 gives:

$$\overline{h\nu} = \begin{cases} 0.62 \text{ MeV for } ^{137}\text{Cs} \\ 1.17 \text{ MeV for } ^{60}\text{Co} \end{cases}$$

assuming values of $h\nu_0$ of 662 keV for ^{137}Cs and 1.25 MeV for ^{60}Co .

